Interaction of granular avalanches with obstacles and topography

C.G. Johnson[1]* and J.M.N.T. Gray[1]

[1] *School of Mathematics and Manchester Centre for Nonlinear Dynamics, The University of Manchester, Oxford Road, Manchester M13 9PL, UK.*

**Corresponding author, e-mail: chris.johnson@manchester.ac.uk*

ABSTRACT

Snow avalanches are strongly influenced by the basal topography that they flow over. In particular, localized bumps or obstacles can generate rapid changes in the flow thickness and velocity (shock waves) that dissipate significant amounts of energy. Understanding how avalanches flow over or around obstacles is therefore very important for the design of catching or deflecting dams. Even the flow over a smooth bump is not as simple as one might expect. At steady state the flow can detach from the obstacle and form an airborne jet, or it can stay attached to the bump by forming an upstream shock. Multiple steady states also form in the oblique flow past a wedge, with either a weak, strong or detached shock forming dependent on the upstream Froude number and the wedge deflection angle. Flows past cylinders generate bow shocks and grain free regions on the lee side, while blunt bodies form an upstream detached shock and a dead zone adjacent to the obstacle. Depth-averaged avalanche models are able to solve for most of these configurations although they are not able to model the airborne jet where the particles follow ballistic trajectories.

1. INTRODUCTION

The first shallow-water-like snow avalanche models were developed in Russia (see e.g. Grigorian et al. 1967) and were motivated by the close analogy between the flow of a shallow layer of snow and a shallow layer of fluid. Savage and Hutter (1989) provided the first formal derivation of a depth-averaged model appropriate for snow avalanches and the theory used in this paper is a generalization of that early work and is a synthesis of the two-dimensional models of Gray, Wieland and Hutter (1999) and Gray, Tai and Noelle (2003). The model is formulated in an orthogonal curvilinear coordinate system $Oxyz$ in which the downslope coordinate x is defined by a curvilinear reference surface that follows the terrain and is inclined at an angle $\zeta(x)$ to the horizontal, the y-axis points across the slope and the z-axis is the upward pointing normal. In these coordinates the depth-averaged mass and momentum balances for the avalanche thickness $h(x,y,t)$ and the depth-averaged velocity $\overline{u}(x,y,t)$ are

$$\frac{\partial h}{\partial t} + \operatorname{div}(h\bar{\boldsymbol{u}}) = 0, \qquad (1)$$

$$\frac{\partial}{\partial t}(h\bar{\boldsymbol{u}}) + \operatorname{div}(h\bar{\boldsymbol{u}} \otimes \bar{\boldsymbol{u}}) + \operatorname{grad}\left(\frac{1}{2}gh^2\cos\zeta\right) = h\boldsymbol{S} - hg\cos\zeta\operatorname{grad} b, \qquad (2)$$

where g is the constant of gravitational acceleration, the operators div, grad and dyadic product $\otimes$ are defined in the (x,y)-surface and z=$b(x,y)$ defines the height of any superposed topography above the curvilinear reference surface. The source term on the right

hand side of (2) is due to the component of gravity acting in the downslope direction $\boldsymbol{i}$ and a Coulomb friction μ that opposes the direction of motion

$$\boldsymbol{S} = g \sin\zeta\, \boldsymbol{i} - \mu(g\cos\zeta + \kappa\bar{u}^2)\frac{\bar{\boldsymbol{u}}}{|\bar{\boldsymbol{u}}|}, \qquad (3)$$

where $\kappa = -\partial\zeta/\partial x$ is curvature of the terrain-following coordinate and which provides a correction to the hydrostatic pressure. The system is hyperbolic and it is therefore useful to define the Froude number $\mathrm{Fr} = |\bar{\boldsymbol{u}}|/\sqrt{g\,h\,\cos\zeta}$, which is the ratio of the flow speed to the gravity wave speed. In particular, the flow is subcritical if $\mathrm{Fr} < 1$, critical if $\mathrm{Fr} = 1$ and supercritical if $\mathrm{Fr} > 1$ in which case shocks (or discontinuities) in the solution are anticipated. In this situation equations (1-2) are no longer valid, because they assume smoothness. Instead it is possible to derive jump conditions (see e.g. Chadwick 1974) for the depth-averaged mass and momentum that apply across the discontinuity

$$[\![h(\bar{\boldsymbol{u}}\cdot\boldsymbol{n} - v_n)]\!] = 0, \qquad (4)$$

$$[\![h\bar{\boldsymbol{u}}(\bar{\boldsymbol{u}}\cdot\boldsymbol{n} - v_n)]\!] + [\![\tfrac{1}{2}gh^2\cos\zeta]\!]\boldsymbol{n} = 0, \qquad (5)$$

where the jump bracket notation is the difference of the enclosed quantity on either side of the shock, $\boldsymbol{n}$ is the normal to the shock and v_n is the shock speed in the normal direction.

2. MULTIPLE STEADY STATES FOR THE FLOW OVER A SMOOTH BUMP

Fig. 1(a,b) shows two different flows over a smooth bump arising from identical upstream conditions (Viroulet et al. 2017). In Fig. 1(a) the avalanche flows rapidly over the bump and forms an airborne jet, while in Fig. 1(b) the avalanche first impacts and then mobilizes a static layer of grains in front of the bump. This allows a normal shock wave to propagate upslope until it finds a stable location. The subsequent oncoming flow is dramatically slowed by the upstream shock and forms a subcritical flow that transitions back to supercritical as it flows over the bump. Importantly, however, the flow does not detach from the obstacle.

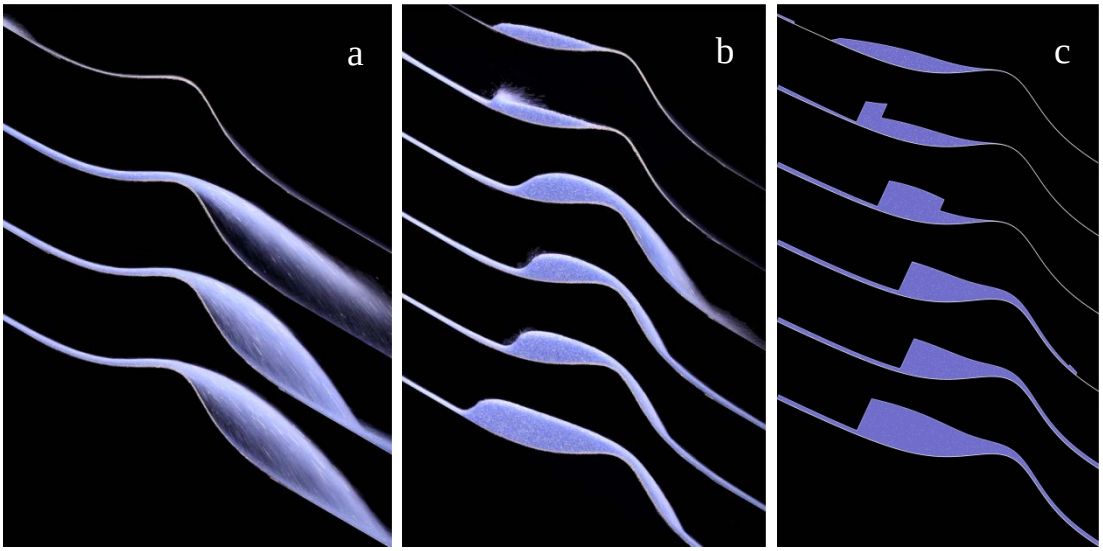

Figure 1 An experimental avalanche flowing over a smooth bump (a,b) for the same upstream Froude number Fr = 7.6. A numerical simulation (c) for the case when there are static grains upstream and a normal shock forms (Viroulet et al. 2017).

The jet and the upstream shock solutions represent two steady states of the system. It is possible to flip between the two, by either momentarily blocking the jet or by scraping away some of the subcritical material. The terrain-following avalanche theory (1-3) is able to predict when the normal traction is equal to zero and hence when the avalanche takes off. The flying grains can then be treated as an inviscid jet (Hákonardóttir et al. 2003; Johnson et al. 2011) or by following the ballistic trajectories of the grains (Viroulet et al. 2017).

It is also possible to derive an exact solution, for the case when a normal shock forms upstream of the bump, using both the terrain-following theory and a more conventional avalanche model in which the height of the topography is prescribed by $z = b(x)$ above an inclined plane at an angle ζ to the horizontal. The critical point ($\mathrm{Fr} = 1$) plays a crucial role in determining a unique position for the steady-state shock in both cases. Unlike some conventional avalanche models the terrain-following theory is able to match the experimental shock position for a wide range of inclination angles, using the same frictional parameters, making this problem a sensitive test case. Using shock-capturing numerical methods (Kurganov and Tadmor, 2000) it is possible to simulate the evolution towards the steady state (Fig. 1c) including the impact with, and mobilization of, the static grains in front of the bump.

3. WEAK, STRONG AND DETACHED OBLIQUE SHOCKS

There are also multiple steady states for the flow of an avalanche past a deflecting wedge as shown in Fig. 2(a,b). For a sufficiently high upstream Froude number Fr_1 and low wedge deflection angle θ (see Fig. 2c) the jump conditions (4-5) imply that the shock deflection angle β can either be small, which is known as weak shock, or large, which is known as a strong shock (Rouse 1938, Ippen 1949, Gray et al. 2003, Hákonardóttir, K. M., Hogg, 2005, Gray and Cui 2007, Vreman et al. 2007, Akers et al. 2008). Weak shocks tend to form naturally if there is no downstream resistance to motion, but strong shocks can be triggered by temporarily blocking the flow or if the constriction is sufficiently small. Strong shocks are potentially very interesting for the design of avalanche protection structures, because the decreases in velocity and the increase in thickness across them is much greater than for weak shocks, so they dissipate a lot of energy. When the incoming Froude number Fr_1 is too low or the wedge angle is too high then there are no steady-state solutions that are attached to the wedge tip and a detached oblique shock forms upstream instead.

4. BOW SHOCKS AND GRAIN FREE REGIONS

For flows around cylinders (Fig. 3) the shock always detaches from the obstacle and forms a bow shock upstream of it. There is a stagnation point on the cylinder, where the velocity is zero, which implies there is a rapid deceleration as the grains as they pass through the shock and the subcritical region upstream of the cylinder. As the grains move around the obstacle the flow becomes supercritical again and expands on the lee side. The internal pressure is not sufficient to immediately push the grains around the lee side of the cylinder and a void opens up that is completely grain free. The lateral pressure gradients pushing in from either side slowly close the void with increasing downstream distance as shown in Fig. 3(a,b). Shock-capturing numerical simulations (Cui and Gray 2013) using the avalanche equations (1-3) on an inclined plane, with a no penetration condition on the cylinder walls, are able to capture the time-dependent development of the flow around the obstacle, as well as the downstream closure of the grain-free region, and closely match the steady-state solution (Fig 3c) .

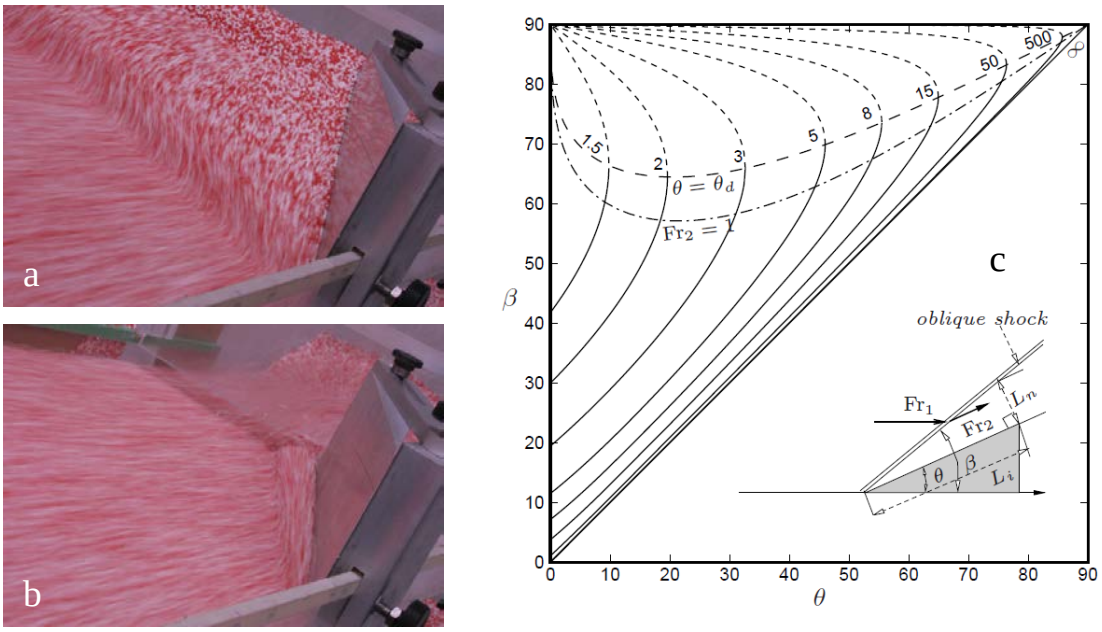

Figure 2 Oblique views of (a) a strong shock and (b) a weak shock for a flow at $Fr_1 = 5$ that is deflected by wedge at an angle $\theta = 20^o$ *(*Gray and Cui 2007). Provided Fr_1 (indicated by the numbers in c) is sufficiently high and the wedge angle θ is low enough, there is either a weak (solid lines) or a strong (dashed lines) solution for the shock deflection angle β. If the incoming Froude number is too low then the shock detaches (Gray and Cui 2007, Cui, Gray and Johannesson 2007*).*

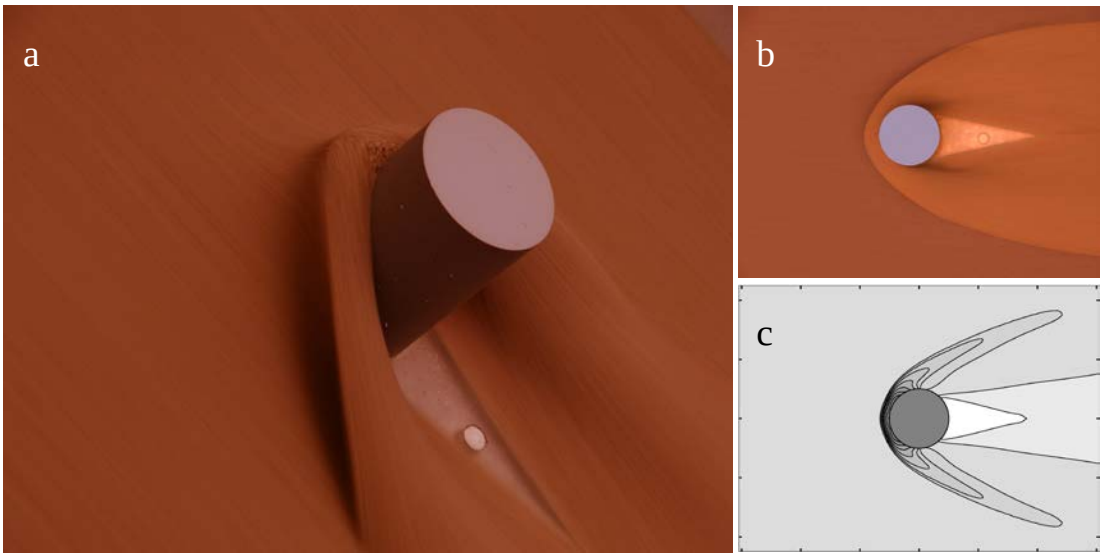

Figure 3 (a) Oblique and (b) overhead views of a supercritical flow of dry sand past a cylinder for $\zeta = 36^{\mathrm{o}}$ and $\mathrm{Fr} = 6$. A bow shock forms upstream of the cylinder and a grain free (vacuum) region forms on the lee side. (c) Computed contours of the avalanche thickness using a depth-averaged avalanche model. The vacuum region is shown in white (Cui and Gray 2013).

5. BLUNT OBSTACLES AND THE FORMATION OF STATIC DEAD ZONES

When the obstacle has a blunt face, the avalanche can spontaneously form a dead zone adjacent to the obstacle, in which there is no flow, as shown experimentally for the pyramidal obstacle in Fig. 4(a,b). As a result the incoming flow is deflected by the dead zone, rather than the obstacle itself, and a detached bow shock then forms upstream. Shock capturing numerical simulations that define the topography in terms of its height $z = b(x, y)$ above the inclined plane are able to quantitatively capture both the formation of the dead zone and bow shock, as well as the fact that most of the grains in the dead zone are left on the upstream face of the pyramid when the flow ceases. The small airborne region of grains flowing over the pyramid faces (Fig. 4a) is not captured by the theory (Fig.4 c), but the predictions for both the flow and the grain free region on the lee side are not adversely affected.

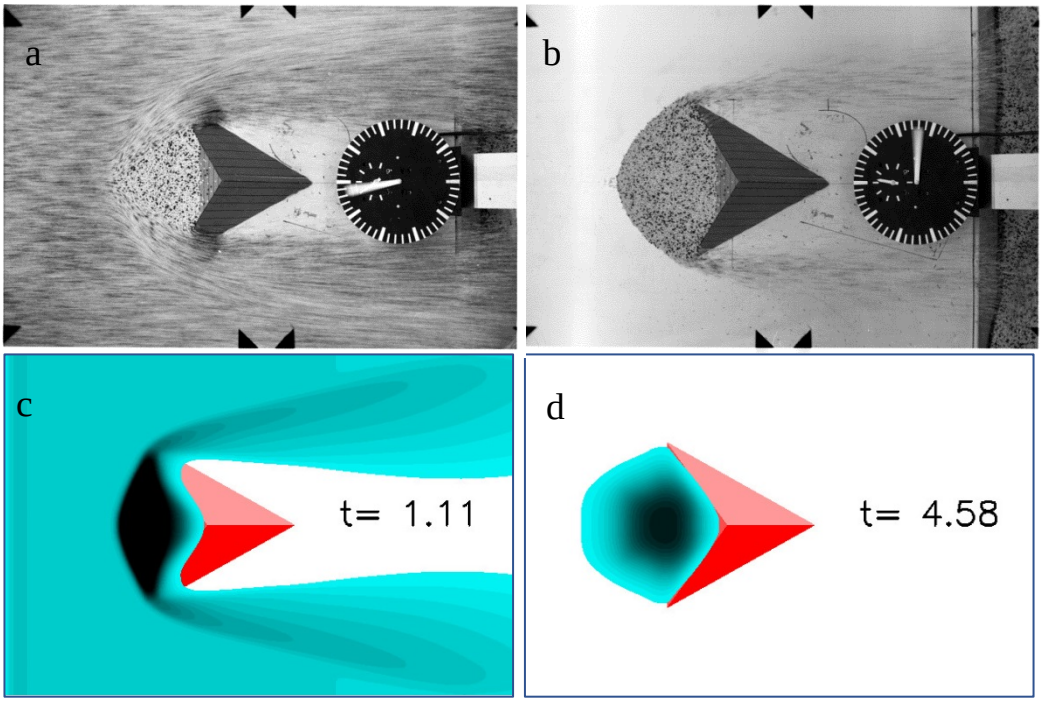

Figure 4 The formation of a shock and a static dead zone (Gray, Tai and Noelle 2003) upstream of the pyramidal obstacle in experiment (a,b) and simulation (c,d). The downslope direction is from left to right.

6. CONCLUSIONS

The depth-averaged terrain-following avalanche equations (1-3) provide a useful framework for computing the flow around many types of obstacle (Gray et al. 1999, 2003, Viroulet et al. 2017). The model is able to realistically capture key phenomena of rapid avalanches, such as multiple steady states and the formation of normal, oblique and detached shocks, grain-free regions as well as static dead zones. The theory can also solve for the point at which a flow will detach from the ground. An inviscid fluid (Hákonardóttir et al. 2003) or ballistic model (Viroulet et al 2017) can be used to solve for the trajectory of the jet. However, there is still much that is not understood about the dissipation that occurs when the jet lands (Johnson and Gray 2011) and forms an avalanche downstream of the obstacle.

ACKNOWLEDGEMENT

This research was supported by NERC grants NE/E003206/1 and NE/K003011/1 as well as EPSRC grants EP/I019189/1, EP/K00428X/1 and EP/M022447/1. J.M.N.T.G. is a Royal Society Wolfson Research Merit Award holder (WM150058) and an EPSRC Established Career Fellow (EP/M022447/1).

REFERENCES

Akers, B., Bokhove, O., 2008. Hydraulic flow through a channel contraction: multiple steady states. Phys. Fluids 20, 056601.

Chadwick, P., 1976. Continuum mechanics. In Concise Theory and Problems. George Allen & Unwin (republished Dover 1999).

Cui, X., Gray, J. M. N. T.. Johannesson T., 2007. Deflecting dams and the formation of oblique shocks in snow avalanches at Flateyri, Iceland. J. Geophys. Res. 112, F04012.

Cui, X., Gray, J. M. N. T., 2013. Gravity-driven granular free-surface flow around a circular cylinder. J. Fluid Mech. 720, 314-337.

Gray, J. M. N. T., Cui, X., 2007. Weak, strong and detached oblique shocks in gravity driven granular free-surface flows. J. Fluid Mech. 579, 113-136.

Gray, J. M. N. T., Tai Y.-C., Noelle S. 2003. Shock waves, dead-zones and particle-free regions in rapid granular free surface flows J. Fluid Mech. 491, 161-181.

Gray, J. M. N. T., Wieland, M., Hutter K. 1999. Free surface flow of cohesionless granular avalanches over complex basal topography. Proc. Roy. Soc. 455, 1841-1874.

Grigorian, S. S., Eglit, M. E., Iakimov, I. L., 1967. New statement and solution of the problem of the motion of snow avalanche. Snow, Avalanches & Glaciers. Tr. Vysokogornogo Geofizich. Inst. 12, 104–113.

Hákonardóttir, K. M., Hogg, 2005 Oblique shocks in rapid granular flows. Phys. Fluids 17, 0077101.

Hákonardóttir, K. M., Hogg, A. J., Batey, J. & Woods, A. W., 2003, Flying avalanches. Geophys. Res. Lett. 30, 2191.

Ippen, A. T., 1949. Mechanics of supercritical flow. ASCE 116, 268–295.

Jóhannesson, T., Gauer, P., Issler, D, Lied, K., (eds.), 2009. The design of avalanche protection dams. Recent practical and theoretical developments. Brussels, Directorate-General for Research, Environment Directorate, European Commission, Publication EUR 23339, 195 pp., doi: 10.2777/12871.

Johnson, C. G., Gray, J. M. N. T., 2011. Granular jets and hydraulic jumps on an inclined plane. J. Fluid Mech. 675, 87-116.

Kurganov, A., Tadmor, E., 2000. New high-resolution central schemes for nonlinear conservation laws and convection-diffusion equations. J. Comput. Phys. 160, 241–282.

Rouse, H. 1938 Fluid Mechanics for Hydraulic Engineers. McGraw-Hill.

Savage, S. B., Hutter, K., 1989. The motion of a finite mass of granular material down a rough incline. J. Fluid Mech. 199, 177–215.

Viroulet, S. Baker, J. Edwards, A. N., Johnson, C. G., Gjaltema, C., Clavel, P., Gray, J. M. N. T., 2017. Multiple solutions for granular flow over a smooth two-dimensional bump. J. Fluid Mech. 815, 77-116.

Vreman, A. W., Al-Tarazi, M., Kuipers, J. A. M., Van Sint Annaland, M., Bokhove, O., 2007. Supercritical shallow granular flow through a contraction: experiment, theory and simulation. J. Fluid Mech. 578, 233–269.